

DFUB 98/17
Bologna, July 1998

Low energy atmospheric ν_μ in MACRO ¹

M. SPURIO (For the MACRO collaboration)

Università di Bologna and INFN - Viale Bertini Pichat 6/2 -40127 Bologna.

Email: spurio@bo.infn.it

Abstract

The flux of low energy neutrinos ($\bar{E}_\nu \sim 4 \text{ GeV}$) has been studied with the MACRO detector at Gran Sasso via the detection of ν_μ interactions inside the apparatus, and of upward-going stopping muons. Data collected in $\sim 3 \text{ y}$ with the full apparatus were analyzed. The results are compatible with a deficit of the flux of atmospheric ν_μ from below, and no reduction from above, with respect to Monte Carlo predictions. The deficit and the angular distributions are interpreted in terms of neutrino oscillations, and compared with the MACRO results on the upward throughgoing muons ($\bar{E}_\nu \sim 100 \text{ GeV}$).

Introduction

Recent results from Super-Kamiokande (Fukuda 98) confirmed the anomaly in the ratio of contained ν_μ to ν_e interactions, suggesting best fit parameters of $\sin^2 2\theta \simeq 1.0$ and Δm^2 in the range of a few times 10^{-3} eV^2 for ν_μ disappearance. Other positive results come from Kamiokande (Fukuda 94), IMB (Casper 91) and Soudan 2 (Allison 97) while earlier results from Frejus (Daum 95) and NUSEX (Aglietta 1989) are consistent with the expected number of contained events with smaller statistics. Also the results from MACRO (Ahlen 95) on up throughgoing muons presented an anomaly.

The MACRO detector (Ahlen 93) is a large rectangular box ($76.6 \text{ m} \times 12 \text{ m} \times 9.3 \text{ m}$) whose active detection elements are planes of streamer tubes for tracking and liquid scintillation counters for fast timing. The lower half of the detector is filled with trays of crushed rock absorber alternating with streamer tube planes, while the upper part is open. The low energy ν_μ flux can be studied by the detection of ν_μ interactions inside the apparatus, and by the detection of upward going muons produced in the rock below the detector and stopping inside the detector (Fig. 1a). Because of the MACRO geometry, muons induced by neutrinos with the interaction vertex inside the apparatus can be tagged with *time-of-flight* (*T.o.F.*) measurement only for upgoing muons (*IU* μ =*Internal Upgoing* μ). The downgoing muons with vertex in MACRO (*ID* μ =*Internal Downgoing* μ) and upward going muons stopping inside the lower part of the detector (*UGS* μ = *Upward Going Stopping* μ) can be identified via topological constraints. Fig. 1b shows the parent neutrino energy distribution for the three event topologies that can be detected by MACRO.

¹Contributed paper for the 16th ECRS - Alcalá de Henares (Madrid) - 20/25 July 1998

Internal Upgoing Events (IU)

The data sample used for the Internal Upgoing (IU) events corresponds to a live-time of 3.16 years from April, 1994 up to November, 1997. During this period, $\sim 22 \cdot 10^6$ atmospheric single muons were collected. The identification of $IU\mu$ events was based both on topological criteria and *T.o.F.* measurements. The basic requirement is the presence of at least two scintillator clusters in the upper part of the apparatus (see Fig. 1a) matching a streamer tube track reconstructed in space. A similar request was made in the analysis for the up throughgoing events (Ambrosio 98).

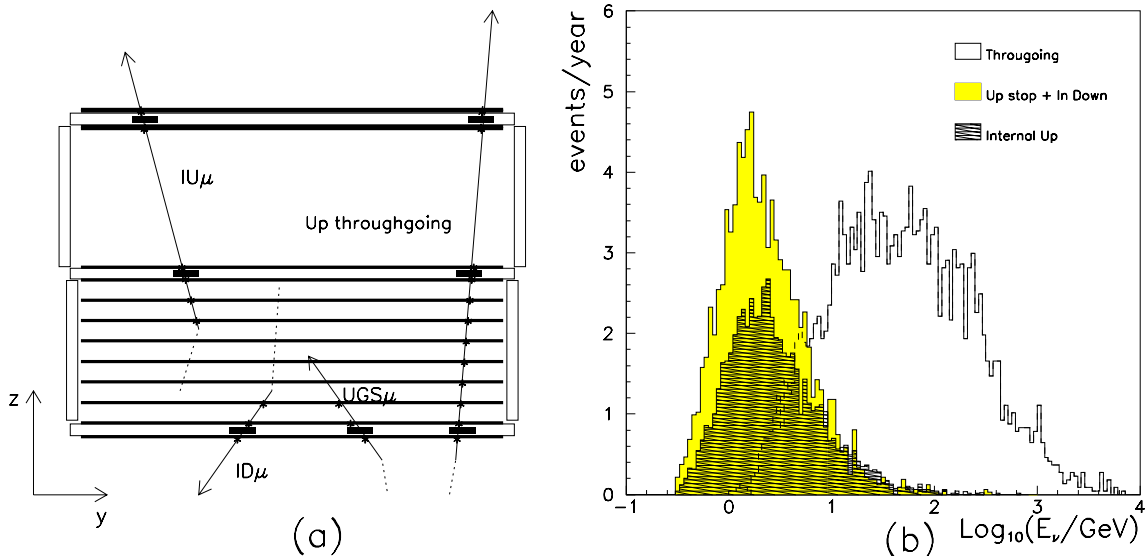


Figure 1: (a) Sketch of different event topologies induced by neutrino interactions in or around MACRO. $IU\mu$ = Internal Upgoing μ ; $ID\mu$ = Internal Downgoing μ ; $UGS\mu$ = Upgoing Stopping μ ; Up throughgoing = upward throughgoing μ . In the figure, the stars represent the streamer tube hits, and the black boxes the scintillator hits. The *time-of-flight* of the particle can be measured for the $IU\mu$ and up throughgoing events. (b) Parent neutrino energy distributions for the three ν_μ samples illustrated in (a).

For $IU\mu$ candidates, the track starting point must be inside the apparatus. To reject fake semi-contained events entering from a detector crack, the extrapolation of the muon track in the lower part of the detector must cross and not fire a minimum number of streamer tube planes and scintillator counters depending on track configuration. The above conditions, tuned with Monte Carlo simulated events, account for detector inefficiencies and reduce the background contribution from upward throughgoing muons, which appear like semi-contained event to $\sim 1\%$. The measured $1/\beta$ distribution is shown in Fig. 2. The measured muon velocity βc is calculated with the convention that downgoing muons have $1/\beta$ values centered at +1 while upgoing muons have $1/\beta$ at -1. It was evaluated that three events are due to an uncorrelated background. After background subtraction, 85 events are classified as IU events.

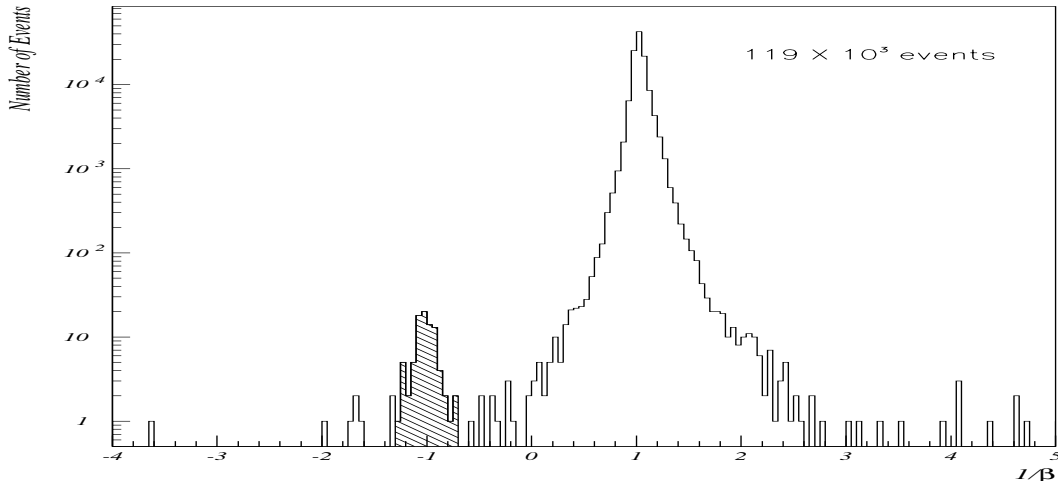


Figure 2: The $1/\beta$ distribution of the 85 IU events (dashed area). The $\sim 1.2 \cdot 10^5$ events centered at $1/\beta = +1$ are downgoing atmospheric stopping muons.

UpGoing Stopping (UGS) and Internal Downgoing (ID) Events

The UGS+ID events were identified via topological constraints, and not with the *T.o.F.* For this analysis, the effective live-time is 2.81 *y.* The main request for the event selection is the presence of one reconstructed track crossing the bottom layer of the scintillation counters (see Fig. 1a). All the hits along the track must be at least one meter inside from each wall of a MACRO supermodule. The selection conditions for the event vertex (or μ stop point) to be inside in the detector are similar to those used for the IU search; they reduce to a negligible level the probability that an atmospheric muon produces a background event. The main difference with respect to the IU analysis (apart the *T.o.F.*) is that on average fewer streamer tube hits are present. To reject ambiguous and/or wrongly tracked events which passed the event selection, a systematic scan with the MACRO Event Display was performed. All real and simulated events which passed the event selection criteria were randomly merged. The finally accepted events had to pass the double scan procedure (the differences are included in the systematic uncertainty). In real events, three different subsamples were considered, according to the number of streamer tube hits, $=NWP$ along the reconstructed track.

	\overline{E}_ν (GeV)	R_{min} ($g\ cm^{-2}$)	ν_μ %	Events	Bck. ($\pm 20\%$)	MC (no osc.)
A (All events)	3.1	30	81	241	22	256
B ($NWP \geq 3$)	3.9	100	90	125	5	159
C ($NWP \geq 4$)	4.9	160	94	66	1	95

Table 1: Summary results (see text) for the three subsamples of ID+UGS events.

As shown in Table 1, each subsample is distinguished by a different average parent

neutrino energy (col. 2); minimum range ($g\text{ cm}^{-2}$) of detector material to be crossed by the neutrino-induced particle (col. 3); percentage of ν_μ C.C. interactions (col. 4). In column 5 are given the numbers of real events.

The main background source is due to upward going charged particles (mainly pions) induced by interactions of atmospheric muons in the rock around the detector (Ambrosio 98). The background affects mainly sample *A*, and becomes smallest in sample *C*, as shown in col. 6 of Table 1. Sample *B* is used in the next section.

Comparisons between Data and Monte Carlo

The expected rates of IU and ID+UGS events were evaluated with a full Monte Carlo simulation. The ν_e and ν_μ were allowed to interact in a large volume of rock containing the experimental Hall B and the detector. The rock and detector mass in the generation volume is 175 kton. The atmospheric ν_μ flux given by the Bartol group (Agrawal 96) and the ν cross sections of (Lipari 94) were used. The detector response was simulated using GEANT, and simulated events are processed in the same analysis chain as the real data. In the simulation, the parameters of the streamer tube and scintillator systems have been chosen in order to reproduce the real average efficiencies. The total theoretical uncertainty for the muon production from ν_μ at these energies is $\sim 25\%$. The systematic error is of the order of 10%, arising mainly from the simulation of detector response, data taking conditions, analysis algorithm efficiency, mass and acceptance of the detector. With our full MC, the prediction for IU events is $144 \pm 36_{\text{theor}} \pm 12_{\text{syst}}$, while the observed events are $85 \pm 9_{\text{stat}}$. The ratio $R = (DATA/MC)_{IU} = 0.59 \pm 0.06_{\text{stat}} \pm 0.15_{\text{theor}} \pm 0.06_{\text{syst}}$.

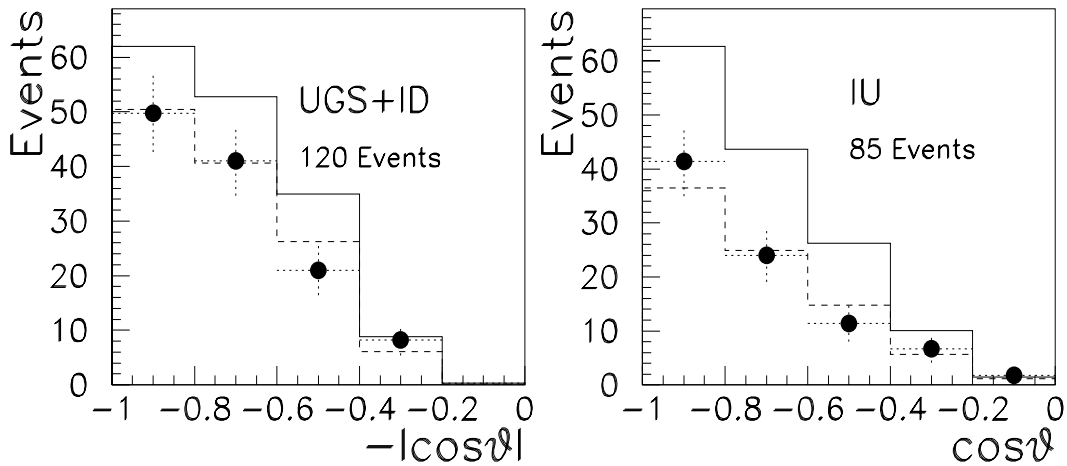


Figure 3: Distribution of the cosine of the zenith angle (θ) for ID+UGS (samples B) and IU events. The background-corrected data points (black points with error bars) are compared with the Monte Carlo expectation assuming no oscillation (full line) and two-flavour oscillation (dashed line) using maximum mixing and $\Delta m^2 = 2.5 \cdot 10^{-3} \text{ eV}^2$.

The MC prediction for ID+UGS events are shown in the last column of Table

1; in particular for sample B we expect $159 \pm 40_{theor} \pm 13_{syst}$ events. The ratio $R = (DATA/MC)_{ID+UGS} = 0.75 \pm 0.07_{stat} \pm 0.19_{theor} \pm 0.08_{syst}$. An almost equal number of ID and UGS neutrino induced events are expected in our data sample. The angular distribution of the IU and ID+UGS data samples, with the Monte Carlo predictions, are presented in Fig.3.

The low energy ν_μ samples show a deficit of the measured number of events in a uniform way over the whole angular distribution with respect to the predictions based on the absence of neutrino oscillations. The measured deficit of low-energy events is in agreement with the MACRO results on the throughgoing events (Ambrosio 98), *i.e.* with a model of ν_μ disappearance with $\sin^2 2\theta \simeq 1.0$ and $\Delta m^2 \sim 2.5 \cdot 10^{-3} eV^2$. In fact, the IU and UGS events have $L \sim 13000 km$, and in the energy range of few GeV the flux is reduced by a factor of two for maximum mixing and $\Delta m^2 \sim 10^{-2} \div 10^{-3} eV^2$. No flux reduction is instead expected for ID events ($L \sim 20 km$). A global analysis of the different data sets is in progress.

References

- M. Aglietta *et al.*, Europhys. Lett. **8** (1989) 611.
V. Agrawal, T.K. Gaisser, P. Lipari and T. Stanev, Phys.Rev. **D53** (1996) 1314.
S. Ahlen *et al.*, (The MACRO coll.) Nucl. Inst. and Meth. **A324** (1993) 337.
S. Ahlen *et al.*, (The MACRO coll.) Phys. Lett. **B357** (1995) 481 .
W. Allison *et al.*, Phys. Lett. **B391** (1997) 491 .
M. Ambrosio *et al.*, (The MACRO coll.), INFN-AE 97/55.
M. Ambrosio *et al.* (The MACRO coll.), hep-ex/9807005 (1998).
D. Casper *et al.*, Phys. Rev. Lett. **66** (1991) 2561.
K. Daum *et al.*, Z. Phys. C. **66** 417.
Y. Fukuda *et al.*, (Kamiokande Collaboration), Phys. Lett. **B335** (1994) 237.
Y. Fukuda *et al.* (Super Kamiokande Collaboration), hep-ex/9807003 (1998).
P. Lipari, M. Lusignoli and F. Sartogo, Phys. Rev. Lett. **74** (1995) 4384.